EUROPEAN LABORATORY FOR PARTICLE PHYSICS

CERN SL/94-46 (AP)

A Study of the Low Emittance Lattice for LEP2

Y.Alexahin*

Abstract

The single particle stability in a low emittance lattice for LEP2 with horizontal phase advance per cell $\mu_x = 135°$ is studied. The dynamic aperture of such a lattice is shown to be very sensitive to quadrupole misalignment. Various methods to reduce horizontal detuning with amplitude are considered with the purpose to avoid the hotizontal tune crossing an integer value. A new version of the low emittance lattice with a vertical phase advance per cell $\mu_y = 56.25°$ is proposed, which has a larger dynamic aperture.

Geneva, Switzerland
July 8, 1994

* On leave from Joint Institute for Nuclear Research, Dubna, Russia

Contents:

1 Introduction

For a maximum luminosity at the LEP2 energy of 90 GeV per beam a substantial reduction in the natural emittance of the beams is needed [1]. With FODO lattice the emittance reaches its minimum at a horizontal phase advance per cell $\mu_x = 3\pi/4=135°$. Returning the LEP lattice to this phase advance from its present value of 90° would at least double the luminosity with the same current and number of bunches at the $W^{\pm}$ energy [1].

A number of optics versions with $\mu_x=135°$ has been synthesized and studied by J.P.Koutchouk. The analysis of the optics with a most promising vertical phase advance per arc cell value $\mu_y=45°$ (see Ref.[1]) revealed its insufficient dynamic aperture due to a high β_y value at the SD sextupoles. Therefore the effort was concentrated on the optics with $\mu_y=60°$ (called the L-optics), which was tested in a short experiment at the end of 1993. The large horizontal tune value ($Q_x=125.23$ in the particular case) and correspondingly large chromaticity lead to a strong nonlinearity of the betatron motion manifested as :

a) large horizontal detuning with amplitude ($\partial Q_x/\partial W_x=-1.3\cdot10^5 m^{-1}rad^{-1}$) driving the injected beam onto the horizontal integer resonance;

b) large width of resonances, both systematic and driven by imperfections;

c) large third order vertical chromaticity of the physics optics ($Q_y'''=1.8\cdot10^6$).

The first two circumstances may account for the negative results of the experiment mentioned.

The main objective of the present study is to analyze the stability properties of the 135/60 lattice and find possible ways to improve it.

2 Nonlinear Properties of the 135/60 Lattice.

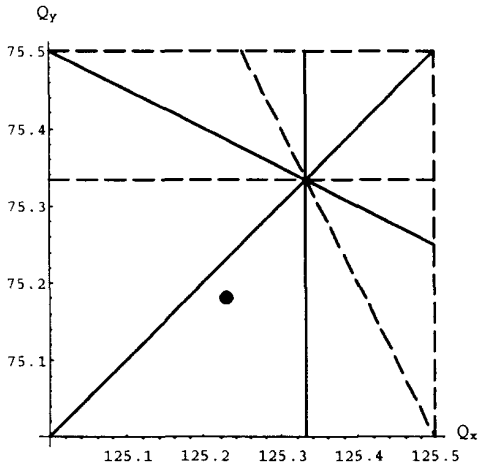

Figure 1. Tune diagram

The working point on the tune diagram chosen for the L-optics ($Q_x=125.23$, $Q_y=75.18$) is shown in Fig.1. This choice of tunes was determined by the fact of reduction in the nonlinear chromaticity for the tunes close to an odd integer in LEP [2], which in the present case is practically the only way to obtain adequate energy acceptance with the physics optics.

The horizontal tune cannot be pulled further away from the integer value (and the 4-th order coupling resonance as well) in the positive direction due to proximity of the third integer systematic resonance $Q_x=125.33$. Tune values below the integer are forbidden by the coherent beam-beam effect [3], therefore the following analysis is confined to the vicinity of the indicated working point.

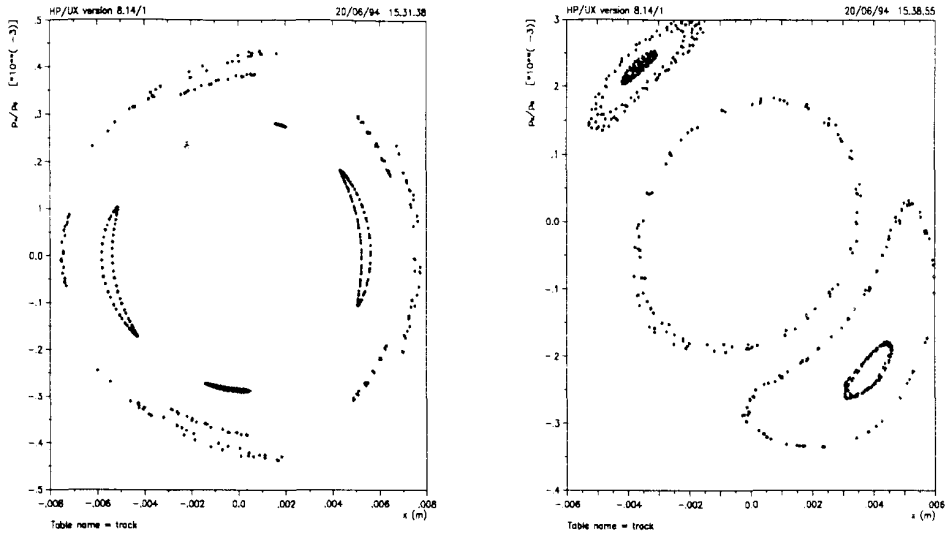

Figure 2. Phase space pattern for the perfect (left) and misaligned (right) machines.

2.1 Detuning with amplitude.

Fig.2 (left) depicts the horizontal phase space pattern in the case of the perfect machine obtained by tracking with the MAD program [3]. Islands corresponding to the fourth, fifth and third integer systematic resonances are clearly seen (appearance of the latter is due to reduction in the effective superperiodicity of LEP at large amplitudes). The coefficient of horizontal detuning with amplitude estimated from these data as[1] $\partial Q_x/\partial W_x \approx \Delta Q_x/W_x$ increases with amplitude in absolute value from $-1.6\cdot10^5 m^{-1}$ to $-1.9\cdot10^5 m^{-1}$, noticeably exceeding the value predicted by the Hamiltonian second order perturbation theory formula incorporated in the MAD routines HARMON and STATIC (which both give practically the same result, see the first row in Table 1). This indicates an appreciable contribution from the higher order terms in the detuning.

2.2 Dynamic aperture with misalignments.

The effect of imperfections on the horizontal betatron motion is illustrated in Fig.2 (right). In this particular case quadrupoles were misaligned to RMS error dx=dy= 0.1 mm and the closed orbit corrected with RMS accuracy of 0.5 mm at pickups in both planes. As expected the four-fold symmetry of LEP was broken and the half-integer resonance structure became prevalent. The large width of the resonant islands testifies to the increased resonance strength. The dynamic aperture in this case is given by the inner trajectory and is approximately four times smaller than that in the ideal case.

To determine the most damaging type of imperfection a short-term tracking (75 turns) has been performed with quadrupoles misaligned to (in MAD notation):

Case 1: dx=dy=0.1 mm, dpsi=0.1 mrad;

Case 2: dx=0.1 mm, dy=dpsi=0;

Case 3: dy=0.1 mm, dx=dpsi=0,

[1] Hereafter W_x and W_y stand for the particle Courant-Snyder invariants.

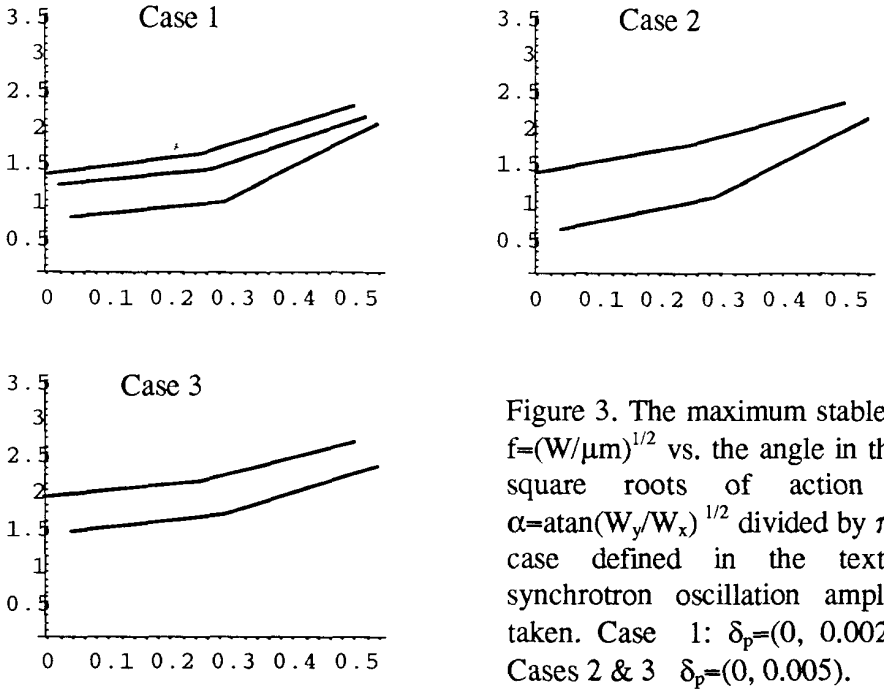

Figure 3. The maximum stable amplitude $f=(W/\mu m)^{1/2}$ vs. the angle in the plane of square roots of action variables: $\alpha=\text{atan}(W_y/W_x)^{1/2}$ divided by π. For each case defined in the text, a few synchrotron oscillation amplitudes are taken. Case 1: $\delta_p=(0, 0.0025, 0.005)$; Cases 2 & 3 $\delta_p=(0, 0.005)$.

and the closed orbit corrected with RMS accuracy of better than 0.5 mm in the x-plane and 1.0 mm in the y-plane. In each case ten different misalignment samples were taken defined by the "seed" value in MAD (i.e. by the position of the first number taken from the random number generator sequence). The tracking data for several synchrotron amplitude (δ_p) values are plotted in Fig.3. The solid lines join mean values over seeds of maximal stable amplitudes $f_{max}=(W_{max}[\text{mm}\cdot\text{mrad}])^{1/2}$ at the same δ_p. Points representing f_{max} at the same α are slightly shifted to avoid overlapping.

It could have been concluded from these data that resonances of horizontal oscillations at Qx=125 are the only factor limiting horizontal dynamic aperture. In fact in many cases particles with a large initial horizontal amplitude and a small vertical one were observed to be lost due to instability of the vertical oscillations.

As follows from the data the particles are insensitive to the vertical misalignment, the reduction in the horizontal dynamic aperture being determined by the horizontal displacement of the quadrupoles. The data obtained with 500-turn tracking for both perfect and misaligned (case (1) with added monitor read errors of .2 mm in both planes) lattices are given in the first row of Table 1. The label l21v1 stands for injection L-optics with β_x^*=5.25m, β_y^*=0.21m at IP2,6 and β_x^*=2.5m, β_y^*=0.21m at IP4,8 in order to reduce coupling in the detector solenoids.

The observed drastic reduction in dynamic aperture due to misalignments, especially in presence of momentum errors, may explain the unsuccessful 1993 result with 135/60 optics.

2.3 Excitation of the pretzels.

The large horizontal detuning in the 135/60 lattice makes operation in the pretzel mode [4] very complicated if at all possible. The difficulties are associated with

Table 1. Detuning and resonance coefficients (as calculated with the MAD STATIC and HARMON routines) and 500 turns dynamic acceptance of the perfect and misaligned lattices with synchrotron amplitudes δ_p=0.0 (upper values) and δ_p=0.005 (lower values) for different lattice configurations at injection energy 20 GeV.

Configuration	$\partial Q_x/\partial W_x$	$\partial Q_x/\partial W_y$	$\partial Q_y/\partial W_y$	R_{3000}	R_{1020}	R_{4000}	R_{2002}	A_x [(π)·mm·mrad]				A_y [(π)·mm·mrad]			
	($\times 10^3$ m^{-1} rad^{-1})							ideal	min	max	mean	ideal	min	max	mean
l21v1	-138	-1	20	2	-8	20	18	2.43	0.56	1.82	0.86	6.92	0.72	4.88	3.36
(135/60)								0.58	0.08	0.36	0.18	5.81	0.25	1.28	0.60
l21v1 in	-139	-1	19	2	-9	20	17	1.42	-	-	-	6.97	-	-	-
pretzel mode								0.24				4.88			
l21v1 +	-16	41	26	60	-44	79	-49	0.20	-	-	-	0.76	-	-	-
pretzel sexts								0.05				0.62			
y21v3	-17	-1	17	-44	20	-15	19	0.14	-	-	-	0.98	-	-	-
(129/61)								0.11				0.62			
l21v1 +	-7	-36	26	0	-12	420	-41	1.00	0.56	1.00	0.78	4.97	1.00	1.44	1.16
SF varying								0.81	0.06	0.72	0.42	4.12	0.56	1.32	0.95
l21v1 +	-26	-49	24	2	-8	?	?	4.54	2.53	3.39	2.90	6.10	2.62	4.54	3.52
cell octups								3.72	1.23	1.72	1.39	3.39	1.46	2.66	2.05
l21v1 +	-130	-2	20	-1	-7	0	43	2.69	0.56	1.21	0.82	6.76	0.72	4.62	2.39
midarc sexts								0.66	0.06	0.42	0.16	4.84	0.20	1.10	0.48
l21v1 +	-129	0	18	4	-7	12	16	2.59	0.64	1.00	0.78	7.78	0.72	4.84	2.40
DISL sexts								0.56	0.04	0.25	0.15	5.76	0.36	1.21	0.75
x21v6	-113	-8	26	11	-11	0	26	5.90	1.00	2.89	1.79	4.54	2.07	4.04	3.16
(135/56)								0.69	0.22	0.53	0.43	3.31	1.02	2.86	1.38
x21v7 +	-65	-13	26	11	-12	?	?	1.54	1.04	1.51	1.22	4.54	1.51	2.10	1.79
LOBS octups								0.86	0.29	0.74	0.45	4.00	1.14	1.69	1.43

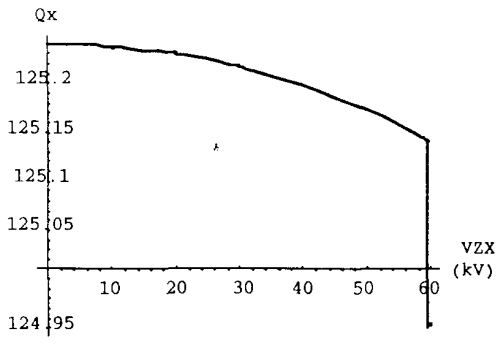

Figure 4. Horizontal tune vs. pretzel separator voltage.

the dependence of the horizontal phase advance between the pretzel separators and overall tunes on the separators voltage (VZX); the latter being shown in Fig.4. At VZX=45 kV which provides pretzel amplitude of 6.2 mm (and the closed orbit displacement in the midarcs of 3.4 mm) the horizontal tune is depressed to Q_x =125.18 leading to a noticeable reduction in the dynamic aperture (Table 1 second row). Therefore a special optics for operation in the pretzel mode should be designed with redistributed phase advances in the dispersion suppressors to increase the orbits separation in the midarcs and a larger Q_x to provide for the tune depression.

2.4 Chromaticity of the physics optics.

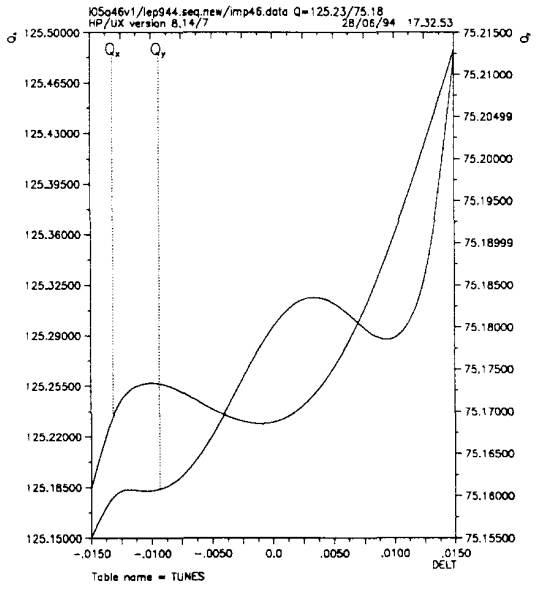

Figure 5. Tunes vs. fractional momentum deviation with optimized excitation of the sextupole families {the third row of Table 2).

Due to the large horizontal phase advance per cell the chromaticity of the physics optics is quite high: with β_x^*= 1.25m, β_y^*= 0.05m the uncorrected values are Q_x'=-247, Q_y'=-188. It should be noted that, because of the relatively large β_y values at SF's (38 m), a high Q_x' leads to an increase in the required strength of *both* SF and SD families. At present there are five sextupole families in the LEP lattice, two SF's and three SD's. With equal excitation of the SD families the energy acceptance of the squeezed optics turns out to be less than ±0.7% which is not sufficient for the beam lifetime. Variation of the SD families excitation [2] permits the compensation of the nonlinear vertical chromaticity (see Table 2 second row) without noticeable deterioration of the dynamic aperture. The energy acceptance is limited then

Table 2. Effect of varying the sextupole families excitation with physics optics.

KSD1	KSD2	KSD3 (m^{-3})	KSF1	KSF2	Q_x'' (10^3)	Q_x''' (10^6)	Q_y'' (10^3)	Q_y''' (10^6)
-0.327	-0.327	-0.327	0.295	0.295	0.454	0.241	5.246	1.820
-0.330	-0.210	-0.453	0.295	0.295	0.479	0.235	0.263	0.010
-0.330	-0.210	-0.453	0.250	0.343	0.717	0.213	0.183	0.007

($Q_{x,y}''$ and $Q_{x,y}'''$ were calculated from the $Q_{x,y}'$ values at δ_p=±1.2%)

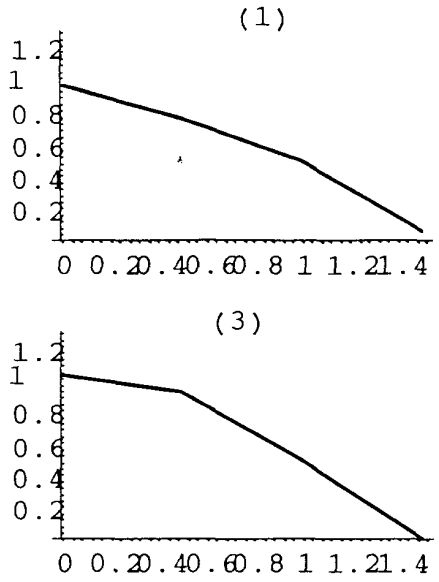

Figure 6. Maximal stable amplitude $f_x=(W_x[\mu m])^{1/2}$ vs. synchrotron oscillation amplitude δ_p [%] with the squeezed optics: (1) l05v1 with equal KSF's; (2) and (3) l05v1 and x05v6 with optimized SF families excitation.

by the chromatic dependence of the horizontal tune which reaches an integer value at δ_p=-0.016. It can be somewhat corrected by varying the SF families excitation (Table 2 third row, see also Fig.5) but at the expense of the on-momentum horizontal dynamic aperture. Fig.6 shows the maximal stable horizontal amplitude dependence on the synchrotron amplitude obtained at E_0=46 GeV by 300 turn tracking with the misalignments as in the subsection 2.2 case (1) and the closed orbit correction RMS accuracy of 0.3 mm in the x-plane and 0.6 mm in the y-plane. Plots 1 and 2 correspond to the sextupole families excitation as given in the Table 2 second and third rows, plot 3 corresponds to the squeezed X-optics which will be discussed in Section 4.

As seen from these data the variation in sextupole strengths needed for compensation of the nonlinear chromaticity is already quite large, so the tunes are really bound to be close to odd integers.

2.5 Conclusions.

- Particle stability in the 135-60 lattice is highly sensitive to imperfections; the horizontal quadrupole misalignment being the most detrimental one.
- The nonlinear vertical chromaticity of the squeezed optics can be easily corrected by varying the excitation of the SD families; the energy acceptance being limited by chromaticity of the horizontal focusing.
- Operation of the 135-60 lattice in the pretzel mode poses serious problems.

3 Possible Methods to Reduce Detuning

As follows from the above analysis the dynamic aperture of the 135-60 lattice in the case of a poorly corrected closed orbit might be insufficient to accommodate the injected beam, especially in the presence of momentum errors. To ensure reproducible injection and sufficient beam lifetime some optics with a larger dynamic aperture is needed. The solution to the problem can be sought for in two ways:

1) reduction of the horizontal detuning with amplitude;

2) cancellation of the betatron resonances limiting the dynamic aperture.

In this section various methods to reduce detuning are considered.

3.1 Correction with the pretzel sextupoles.

The MSX sextupoles installed in the odd pits for e^-/e^+ tune split correction [4] may also (when powered symmetrically) be employed to control detuning and resonance excitation. The SD.QL9's have a larger effect on the horizontal detuning and with k2=2.2 m^{-3} eliminate it almost completely. But the net effect on the dynamic aperture proves to be a highly detrimental one (see the Table 1 third row) due to excitation of nonlinear resonances and strong dependence of detuning on the momentum: as it can be deduced from the MAD STATIC routine output at $\delta_p \neq 0$ in the present case $\partial^2 Q_x/\partial W_x \partial \delta_p \approx -3 \cdot 10^7 m^{-1}$.

3.2 Variation of the arc cell phase advances.

The negative effect of the MSX sextupoles on particle stability is quite typical for a *localized* correction when a few correctors should compensate for the coherent effect of a large number of the arc sextupoles. Therefore a method of *distributed* correction should be sought for. As such variation of the arc cell phase advance and the SF families excitation can be considered.

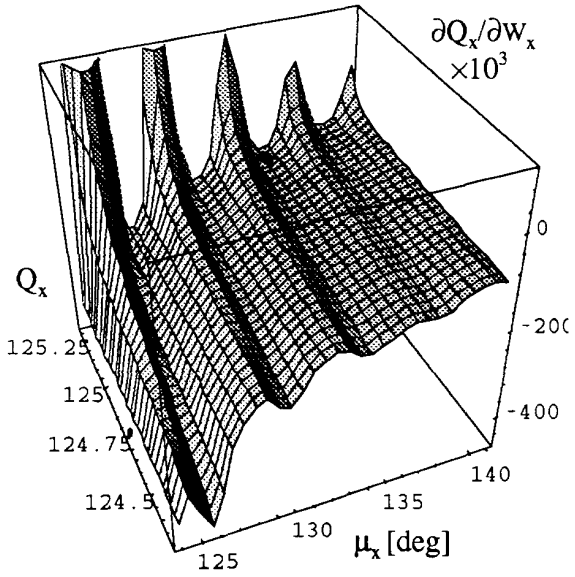

Figure 7. Dependence of the horizontal detuning coefficient on the arc cell phase advance and the tune.

To study the dependence of detunings and resonance driving terms on the arc cell phase advance a Mathematica [5] notebook has been written (see Appendix 2) based on second order perturbation theory. The surface plot in Fig.7 shows the detuning coefficient $\partial Q_x / W_x$ as a function of the horizontal phase advance per cell μ_x and the horizontal tune Q_x with the SF strength, β_x at the SF's and phase advance between an odd IP and the nearest SF being fixed. The dot corresponds to the L-optics working point. On the plot there is a steep crest at μ_x=129.53°. An optics labelled as Y-optics with this μ_x and μ_y=61.45° (chosen to zero $\partial Q_y/\partial W_x$) has been synthesized and examined. (see the Table 1 fourth row). The chosen tune values Q_x=121.23, Q_y=75.18 are modulus 4 equivalent to those of the L-optics. The horizontal dynamic aperture appeared to be extremely small even in absence of misalignments, which could have been predicted from the increased third-order resonance driving terms.

Fig.8 shows that there is a strict correlation between the $|\partial Q_x/\partial W_x|$ minima and the $|R_{3000}|$ maxima for μ_x>120° whereas for μ_x<120° both these values can be kept small simultaneously, with 108° being close to one of the minima. The most striking feature of the Y-optics is a large contribution of the higher order terms in the normalized Hamiltonian. It can be deduced from the tracking data that $\partial^2 Q_x/\partial W_x^2 \approx 2 \cdot 10^{11} m^{-2}$ so that the detuning at $W_x \sim 1$ mm·mrad appears even larger than it was in the L-optics. Therefore an analytical tool taking into account the higherorder terms should be developed to actually reduce detuning by this method.

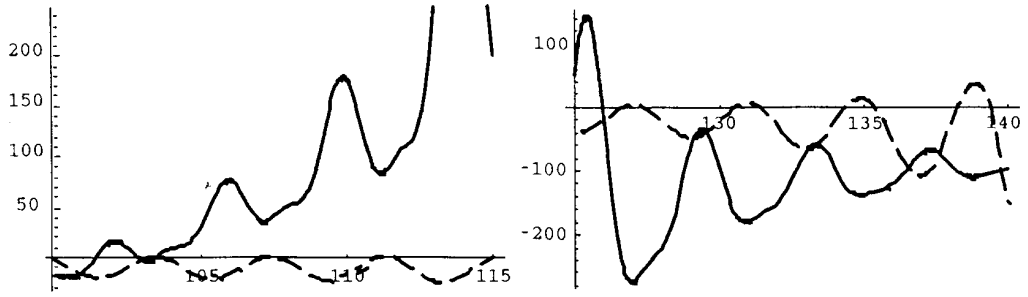

Figure 8. Horizontal detuning and resonance coefficients ($\partial Q_x/\partial W_x \times 10^3$ and R_{3000}) as functions of the horizontal phase advance per cell μ_x with all the other parameters fixed.

3.3 Variation of the SF families excitation.

At present there are two SF families in the LEP lattice (SSF1 and SSF2). Varying the strength of one family and adjusting the other so as to retain the desired linear chromaticity ($Q_x'=Q_y'=2$) one can change not only the nonlinear chromaticity but also the detuning with amplitude. Fig.9 shows the horizontal detuning with amplitude coefficient as a function of SSF1 sextupoles strength. It turns out to be zero at two KSF1 values. Tracking indicates a drastic reduction in the horizontal dynamic aperture at the lower value. At the upper value there is also some reduction, the tracking data for both the perfect and misaligned machines being given in the Table 1 fifth row.

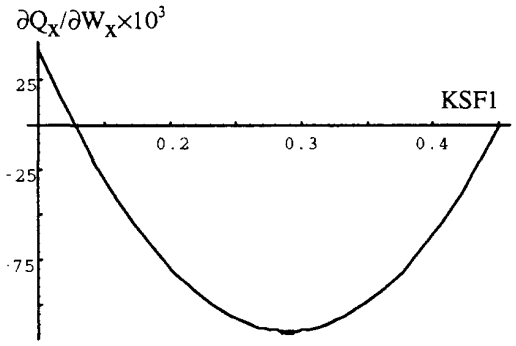

Figure 9. Effect of varying KSF's on the detuning.

Since the strength of the SSF2 family (0.1 m^{-3}) is substantially reduced the effect of varying KSF's can be understood as doubling the phase advances between acting SF sextupoles. With $\mu_x=3\pi/2$ (i.e with $4\mu_x=6\pi$) a drastic enhancement of the 4th integer resonance should be expected, which is confirmed by the MAD HARMON routine (see Table 1). This provides a possible explanation of the observed reduction in the horizontal dynamic aperture.

3.4 Correction with the insertion octupoles.

Though the localized correction of the detuning hardly can improve the dynamic aperture it is instructive to examine the effect of the insertion octupoles located close to the normally idle QS2 quadrupoles. In the standard injection optics contribution from these octupoles to the detuning is relatively small due to a low β_x value at their location (about 150m). This value can be increased by squeezing β_x at the even IP's and using QS2's rather than QS1's for the horizontal focusing. Such an attempt has been made with the X-optics which will be described in the next section.

With $\beta_x^*=2.5$ m and KQS2.2,6=.02 m^{-2}, KQS2.4,8=.025 m^{-2} the β_x value at the octupoles is as high as 300 m which permits to cut the horizontal detuning with amplitude by half at the maximal excitation (K3=17.28 m^{-4} at 20 CeV). Tracking shows a minor reduction in dynamic aperture of the misaligned machine due to the octupoles (Table 1 last row).

3.5 Installation of octupole correctors in arc cells.

It can be argued whether at all it is possible to eliminate the detuning without spoiling the particle stability. To elucidate the point a hypothetical lattice has been examined with thin octupole correctors near each QF quadrupole. With the horizontal phase advance under consideration ($4\mu_x=3\pi$) contributions to the 4th integer resonance from the adjacent correctors cancel, so a good stability should be expected. The Table 1 sixth row presents data obtained with the corrector integrated strength K3L=1.5 m^{-3}.

As can be easily seen this method of correction provides by far the largest dynamic aperture of the misaligned machine confirming in principle the possibility of improving the particle stability by reducing the horizontal detuning with amplitude.

3.6 Conclusions.

- With the existing multipole correctors it is impossible to improve the single particle stability by reducing the horizontal detuning with amplitude. On the contrary all such attempts lead to a strong deterioration of the dynamic aperture.
- To realize the possibility of reducing detuning by varying the phase advance per cell an analytical tool implementing a higher order Hamiltonian perturbation theory is needed.

4 Intrinsic Cancellation of Geometric Aberrations.

As follows from the above analysis at present there is no viable method to reduce detuning and avoid crossing the resonant value $Q_x=125$ at large horizontal amplitudes, therefore some measures should be taken to weaken the resonance excitation. It is substantially reduced when all the sextupoles are arranged in pairs with the combinations of phase advances between them

$$\mu_x, \quad 3\mu_x, \quad \mu_x \pm 2\mu_y \qquad (1)$$

being odd multiples of π [6]. In this respect the following was considered:

a) adding SF sextupoles;

b) changing vertical phase advance per cell to reduce nonlinear coupling;

c) adjusting horizontal phase advances so as to double the lattice effective superperiodicity.

4.1 Effect of additional SF sextupoles.

The two SF families in LEP (SSF1 and SSF2) have in total 31 sextupoles, so the intrinsic cancellation of their kicks cannot be achieved whatever the cell phase advances are. With $\mu_x=3\pi/4$ a horizontally non-aberrant group comprises 8 sextupoles, so one extra SF sextupole in each octant is needed. It can be placed either in the midarc instead of the CH.QF49 corrector or in one of the two dispersion suppressors.

In the first case almost exact cancellation of horizontal kicks is obtained since μ_x varies slowly around QF's, but the arrangement on the whole loses its regularity. In the second case the cancellation is not exact since the betatron functions behave differently in the dispersion suppressors. The error in μ_x is smaller when the additional SF is inserted in DISL, the phase advance between it and the SF.QF19 being about 0.71π. To compensate for a lower β_x value at QL17 the additional sextupole strength should be approximately 1.4 times higher than that of the SSF2's.

The data obtained in these two cases is presented in the Table 1 seventh and eighth rows. Only slight improvement for the perfect machine and no improvement at all in presense of misalignments has been observed in both cases.

4.2 Lattice with compensated nonlinear coupling.

It has been mentioned earlier that in many cases particles with large initial horizontal amplitude were observed to be lost due to instability of the vertical oscillations which can be attributed to the uncompensated nonlinear coupling. With $\mu_x=3\pi/4$, $\mu_y=\pi/3$ a non-aberrant in both planes group comprises 24 sextupoles, so adding one extra SF sextupole per octant does not improve the situation.

The obvious solution would have been to choose the vertical phase advance per cell value $\mu_y=\pi/4$, in which case all combinations (1) become odd multiples of π for the same sextupole pair thus ensuring exact cancellation of its kicks. But this is overcome by the increase in β_y at the sextupoles rendering the net effect negative [1]. With a nearby to $\pi/3$ value of $\mu_y=5\pi/16$ μ_x and $\mu_x \pm 2\mu_y$ become odd multiples of π for different sextupole pairs making an (approximately) non-aberrant group of 16 sextupoles (so again only one SF sextupole is missed in each octant).

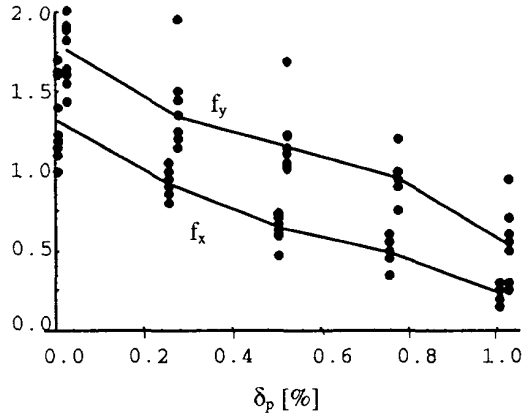

Figure 10. The injection X-optics dynamic aperture.

The data obtained with $\mu_x=3\pi/4$, $\mu_y= 5\pi/16$ optics (called X-optics) are given in the Table 1 ninth row. Another measure which was implemented in this optics and proved to be quite efficient with the injection configuration was equalization of horizontal phase advances between the midarc sextupoles SF.QF49 and the adjacent IP's doubling the lattice effective superperiodicity. As seen from the Table 1 the injection X-optics horizontal acceptance is significantly larger than that of the L- optics. Fig. 10 shows maximal stable amplitudes $f_{x,y}=(W_{x,y}\ [\text{micron}])^{1/2}$ as functions of the synchrotron amplitude in presence of misalignments.

Table 3. Nonlinear chromaticity of the physics X-optics.

KSD1	KSD2	KSD3 (m^{-3})	KSF1	KSF2	Q_x'' (10^3)	Q_x''' (10^6)	Q_y'' (10^3)	Q_y''' (10^6)
-0.317	-0.317	-0.317	0.298	0.298	1.010	0.164	1.210	0.890
-0.320	-0.230	-0.401	0.330	0.263	0.575	0.153	0.113	0.098

($Q_{x,y}''$ and $Q_{x,y}'''$ were calculated from the $Q_{x,y}'$ values at $\delta_p=\pm1\%$ in the first row case and $\delta_p=\pm1.2\%$ in the second one).

Another important feature of the X-optics is a smaller third order vertical chromaticity of the squeezed optics (see Table 3). Without SD-varying the energy acceptance is ±1%. To further increase the energy acceptance a minor rearrangement of the SD-families around midarcs is needed, the resultant grouping SD's in an instance of the second octant is given in the Table 4. The diagram in Fig 11 shows direction of the SD sextupoles kicks on an off-momentum particle in the vertical chromatic functions space [6]. Though the kicks from sextupoles belonging to one family are not exactly in phase, varying the SD's excitation is just as effective as in the $\mu_y=60°$ case, whereas correction of the horizontal nonlinear chromaticity proved to be a more difficult problem.

Table 4. Grouping SD sextupoles in families in the second octant.

SD1	SD2	SD3
SD.QS18.R2	SD.QD20.R2	SD.QD22.R2
SD.QD24.R2	SD.QD26.R2	SD.QD28.R2
SD.QD30.R2	SD.QD32.R2	SD.QD34.R2
SD.QD36.R2	SD.QD38.R2	SD.QD40.R2
SD.QD42.R2	SD.QD44.R2	SD.QD46.R2
SD.QD48.R2		
SD.QD48.L3		
SD.QD46.L3	SD.QD44.L3	SD.QD42.L3
SD.QD40.L3	SD.QD38.L3	SD.QD36.L3
SD.QD34.L3	SD.QD32.L3	SD.QD30.L3
SD.QD28.L3	SD.QD26.L3	SD.QD24.L3
SD.QD22.L3	SD.QD20.L3	SD.QL18.L3

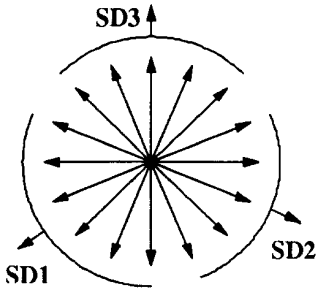

Figure 11. Phases of the SD kicks in the chromatic functions space.

There is another drawback with the present version of the physics X-optics: due to the superperiodicity 8 the $3Q_x$=376 (=8×47) systematic resonance is enhanced so the working point should be pulled farther away from this resonance to allow for the beam-beam tune shift. It might be possible to reduce both this resonance excitation and the horizontal nonlinear chromaticity by redistributing horizontal phase advances between the mid-arcs and IPs during the ramp and squeeze.

5 Summary.

- Strong nonlinearity in the 135/60 lattice poses serious problems due to large detuning with amplitude and nonlinear chromaticity. The injection optics provides dynamic aperture which is marginal for accomodation of the injected beam.
- Attempts to improve the horizontal dynamic aperture by reducing the detuning with amplitude proved to be unsuccessful due to enhancement of betatron resonances. Still there is a possibility to optimize detuning at large amplitudes by a purposeful variation of the second derivatives of tunes.
- The physics 135/60 optics provides at 46 GeV the horizontal dynamic aperture of $12\sigma_x$ with the closed orbit corrected to δx_{RMS}=0.3 mm, δy_{RMS}=0.6 mm at pickups. The energy acceptance is limited to ±1.6% due to the horizontal chromaticity.
- The 135/56.25 optics promises a better dynamic aperture, especially at injection, and practically the same energy acceptance at physics configuration. Still there is a possibility to improve the latter characteristics.

6 Acknowledgements.

The author is grateful to the SL/AP group for the hospitality and support and especially to J.M.Jowett, J.P.Koutchouk and A.J.Verdier for many helpful discussions and ideas.

References

1. J.P.Koutchouk, 'A Superlow Emittance Lattice for LEP2', Proc. 3rd Workshop on LEP Performance, Chamonix, 1993, Ed. J.Poole, CERN SL/93-19(DI), p.511(1993)
2. A.Verdier, 'Chromaticity', Proc. CAS 4th Advanced Accelerator Physics Course, Noordwijkerhoût, Netherlands, 1991, Ed. S.Turner, CERN 92-01, p.204 (1992).
3. H.Grote, F.C.Iselin, The MAD Program. Version 8.10. User's Reference Manual. CERN/SL/90-13(AP) (Rev.3), Geneva, 1993.
4. J.M.Jowett, 'Operation in 1992: Beam Dynamics Aspects', Proc. 3rd Workshop on LEP Performance, Chamonix, 1993, Ed. J.Poole, CERN SL/93-19(DI), p.381(1993)
5. S. Wolfram, Mathematica: A System for Doing Mathematics by Computer. 2nd ed. (Addison-Wesley Publishing Company, 1993).
6. B.Autin, F.Willeke, 'Second Order Tune Shift in a Compensated Super Cell', Proc. 2nd Advanced ICFA Beam Dynamics Workshop, Lugano, 1988, Ed. J.Hagel, E.Keil, CERN 88-04, p.192 (1988).
7. B.W.Montague, 'Chromatic Effects and Their First Order Correction', Proc. CAS Advanced Accelerator Physics Course, Oxford, 1985, Ed. S.Turner, CERN 87-03, p.75 (1987).
8. J.M.Jowett, 'Dynamic Aperture for LEP: Physics and Calculations', Proc. 4th Workshop on LEP Performance, Chamonix, 1994, CERN/SL/94-06 (DI), p. (1994).
9. L.Michelotti, 'Introduction to the Nonlinear Dynamics Arising from Magnetic Multipoles', FERMILAB-Conf-86/30, FNAL, Batavia, 1986.

Appendix 1.
Running MAD via Mathematica for Dynamic Aperture Calculation

■ Introduction

Though many analytical methods exist for analysis of particle stability in circular accelerators tracking still remains the most reliable tool. Unfortunately the tracking codes have a limited flexibility not permitting to implement algorithms for purposeful search of the stability boundary (dynamic aperture) - for instance the MAD program [3] does not support nested DO loops and conditionals.

This inconvenience can be circumvented by using Mathematica [5] as a guide for MAD, preparing input for it, analyzing the output and representing the final result. Hereafter an example is given of establishing *unstructured communication* between Mathematica and MAD for statistical analysis of a misaligned accelerator stability properties.

■ Tracking with misalignments

Since the real imperfections can be determined with but a limited accuracy a number of possible error distributions (determined in MAD by the random generator **seed**) should be taken to obtain reliable results. It is particularly important for low emittance (hence highly nonlinear) lattices of the electron (positron) storage rings since small variation in phase advances between sextupoles due to imperfections destroy compensation (if any) of their kicks and substantially reduce the dynamic aperture.

```
seeds=Table[ 10000*i,{i,10}]; nSeeds=Length[ seeds ];
```

■ Auxiliary Files

The program requires two auxiliary files for MAD input preparation:

- '**jobname**'.**latt** specifying the lattice, misalignments type and closed orbit correction procedure to be studied, where the '**jobname**' stands for a name chosen by the user, and

- **track.proto** formulating the tracking task for MAD.

Both files are assumed to reside in the working directory, The lattice file should be provided by the user, an example can be seen below as an input echo. Output is stored in the file '**jobname**'.**out**.

```
jobname="lep2"; machine=StringJoin[ jobname,".latt"];
                    results=StringJoin[ jobname,".out"];
```

■ Variables and Units

3D dynamic aperture [8] can be represented as a surface in action space. For coordinates are chosen: the synchrotron oscillation amplitude in the form of fractional momentum deviation **deltap**, angle in the plane of (the square roots of) the transverse action variables (divided by π so that **angle**=0 corresponds to purely horizontal and **angle**=0.5 - to purely vertical motion), and the maximal stable amplitude **f** (the square root of the sum of action variables taken in (π)·*mm*·*mrad*).

```
deltaps=.001 {0,2.5,5}; nDelts=Length[ deltaps ];
actionPlaneAngles={0.,.25,.5}; nAngles=Length[ actionPlaneAngles ];
```

■ Algorithm for finding dynamic aperture

Algorithm for finding dynamic aperture is illustrated by the flow diagram in the Fig. A1. The MAD program is called:

- to assemble the lattice, assign imperfections and correct closed orbit for each value of **seed**, saving the configuration on the file **pooldump**;

- to perform tracking with specified by the Mathematica values of **deltap**, **angle**, number of amplitudes **nampl**, the initial amplitude **f0** and **step.**

At each of the latter calls MAD tracks **nampl·nphase** particles with **nampl** amplitudes incremented by **step** from the initial value **f0**. Number of particles with the same amplitude (but different betatron phases) **nphase** corresponds to the number of the START commands in the **track.proto file.** It is set presently to 3 to avoid mistaking stable resonant islands for the dynamic aperture.

When a good guess can be made on the dynamic aperture size it can be found from the first call (especially with the fastest METHOD= TRANSPORT in the MAD TRACK routine). But with a wide scatter due to imperfections this may require too large a **nampl** (and so the CPU time) to cover the possible range of amplitudes with a **step** rendering the desired accuracy. Therefore the search could be done in a larger number of calls **ncalls** with a decreasing **step.**

```
ncalls=2; nphase=3; nampl=19;
mach=ColumnForm[ ReadList[ machine, Record]]

      option,-warn,-ECHO,-info
      !-- Load the machine configuration
      call,'/users/slath/machines/lep94/lep944.seq'
      call,'/users/slath/machines/135-56/md135-56v1.config'
      call,'/users/alexahin/madtools/track/colli.wdn'
      beam,energy=20
      !-- Switch off sextupoles for primary orbit correction
      set,KSD10 KSD1
      set,KSD20 KSD2
      set,KSD30 KSD3
      set,KSF10 KSF1
      set,KSF20 KSF2
      ksd1=0
      ksd2=0
      ksd3=0
      ksf1=0
      ksf2=0
      use,lep
      !-- Specify imperfections and orbit correction
      EOPT,seed=&
      s
      call,'/users/alexahin/lep2/error.defs'
      error.x=.0005
      error.y=.001
      correct,ncorr=32,iter=2,error=error.x,plane=x
      correct,ncorr=32,iter=2,error=error.y,plane=y
      !-- Switch on the sextupoles
      set,KSD1 KSD10
      set,KSD2 KSD20
      set,KSD3 KSD30
      set,KSF1 KSF10
      set,KSF2 KSF20
      correct,ncorr=32,iter=2,error=error.x,plane=x
      correct,ncorr=32,iter=2,error=error.y,plane=y
      !-- Switch on RF and radiation
```

```
      call,'/users/jowett/lep2/RF/rf0.lep'
      beam,bunched,radiate
      emit
      beam,ex=1.e-6,ey=1.e-6,et=1.e-6
      pooldump
      stop

track=ColumnForm[ ReadList[ "track.proto", Record]]

      option,-warn,-echo
      poolload
      ! Insert start data
      f0=&
      f
      step=&
      s
      angle=&
      a
      delt=&
      d
      set,f,f0
      set,cs,cos(angle*pi)
      set,sn,sin(angle*pi)
      track,rfcavity=aas,damp
      set,ft0,delt/beam[sige]
      do,times=&
      n
      set,f,f+step
      set,fx0,f*cs
      set,fy0,f*sn
      start,ft=ft0,fx=fx0,fy=fy0
      start,ft=ft0,fx=fx0,fy=fy0,phix=0.125,phiy=5/12
      start,ft=ft0,fx=fx0,fy=fy0,phix=5/12,phiy=0.125
      enddo
      run,turns=500
      endtrack
      stop

inQ[x_String]:=StringMatchQ[x,"*Particle(s) lost*"];

Do[ seed=seeds[[ iseed ]];
latt=OutputForm[ mach/. "s"->seed]; latt>>"!mad"; Clear[latt];
    Do[ deltap=deltaps[[ idelt ]];
        Do[ angle=actionPlaneAngles[[iang]]; step=.2; f0=0.;
            Do[ task=OutputForm[track/. ["a"->angle, "d"->deltap,
            "f"->f0, "s"->step, "n"->nampl]]; task>>"!mad";
            Clear[task]; mess=ReadList["print", Record];
            npl=Flatten[Position[Map[inQ,mess],True]];
            lnpl=Length[npl]; losp={};
                Do[ (* store lost particles numbers in losp *)
                fw=ToExpression[ First[ ReadList[
                StringToStream[mess[[npl[[i]]+2]] ],Word]]];
                If[ NumberQ[fw], AppendTo[ losp,fw], Continue[]],
                {i,lnpl}]; Clear[mess]; If[ NumberQ[Min[losp]],
            (f0=f0+Floor[ (Min[losp]-1)/nphase]*step; step/=nampl+1),
            f0=f0+nampl*step], {ncalls}];   (* f  found *)
         rest=OpenAppend[results];
         Write[rest,{ seed, deltap, angle, f0}]; Close[ rest],
         {iang,nAngles}],
     {idelt,nDelts}],
{iseed,nSeeds}];

Exit[]
```

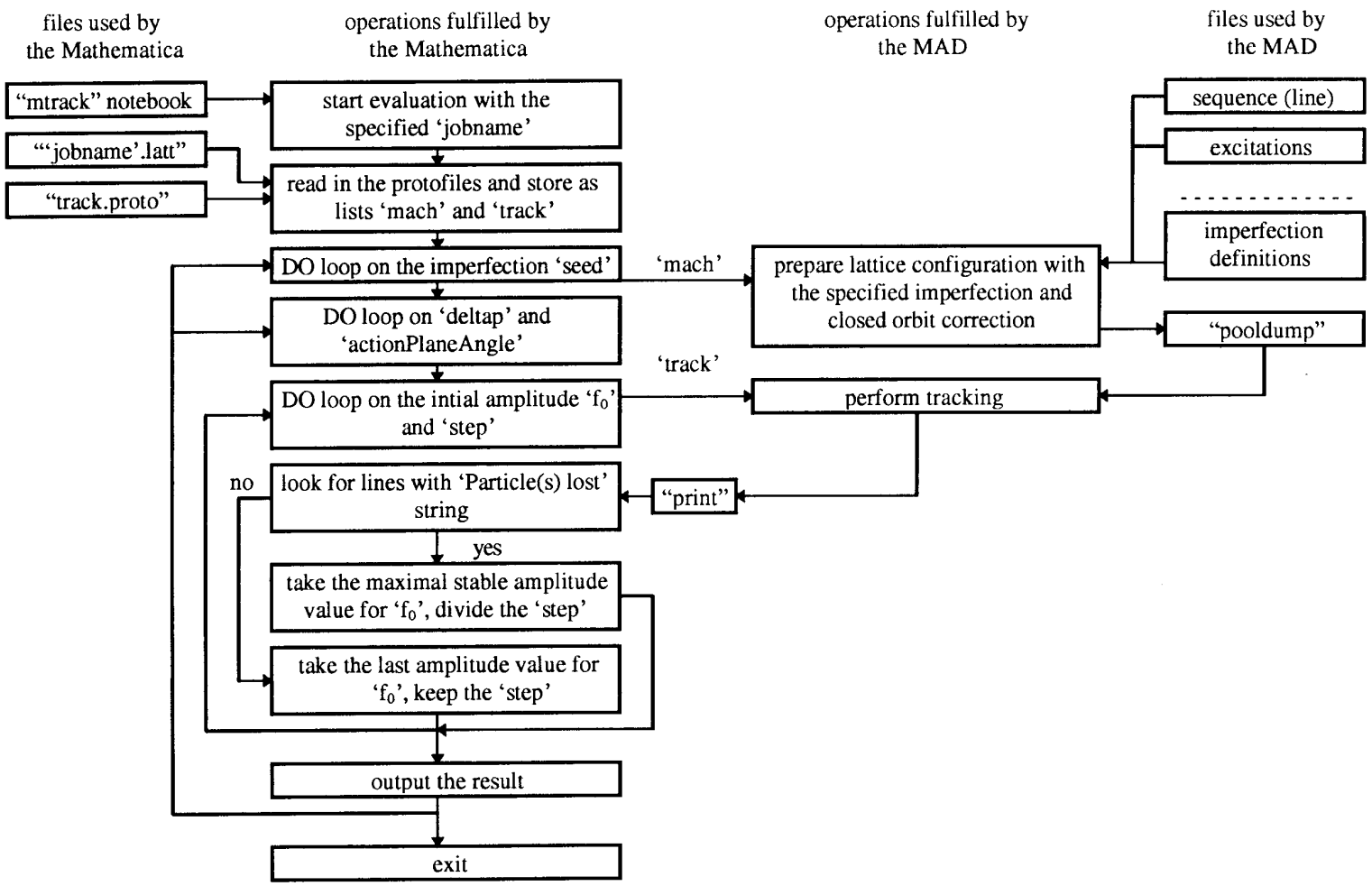

Fig. A1. Flow diagram of the dynamic aperture calculation process

Appendix 2.
Hamiltonian Second Order Perturbation Theory Formulae for a Two Families Sextupole Arrangement

The purpose of this notebook is to provide an analytical tool for studying nonlinear betatron oscillations. It is based on the Hori-Deprit normalization procedure in the form suggested by L.Michelotti [9]. At present the consideration is limted to the second order in the sextupole strength. detuning coefficients and the linear in the sextupole strength resonance driving terms.

The arrangement consists of two interleaved sextupole families (S1 and S2) of ns1 and ns2=ns1+1 sextupoles per half the superperiod reflected w.r.t. the symmetry point theta=Pi. It is assumed that the phase advances between two adjacent sextupoles belonging to different families are half those between sextupoles of the same family.

■ Variables and units

Number of superperiods:

```
nsuper=4;
```

Betatron tunes per a superperiod :

```
q:={qx,75.18}/nsuper;
```

Phase advances per cell [deg]&[rad] :

```
mudeg:={mux,muy}; mu:=mudeg*Pi/180; muy=60;
```

Phase advances from IP to the first S1-sextupole [rad] :

```
phi1={2.276*2*Pi, 1.945*2*Pi}; phi2:=phi1-.5 mu;
```

Betatron functions [m] at the S1 and S2 sextupoles:

```
bx1=169; by1=38; bx2=11; by2=167;
bx12=Sqrt[bx1*bx2]; by12=Sqrt[by1*by2];
```

Integrated sextupole strength [m^-2]

```
k211=.2765*.4; k212=-.2585*.76;
```

Number of sextupoles:

```
ns1=31; ns2=ns1+1;
```

Mode numbers:

```
m[1]={1,0}; m[2]={1,2}; m[3]={1,-2}; m[4]={3,0};
pmq[i_]:=Pi m[i].q; mm[i_]:=m[i].mu;
```

■ Detuning with amplitude

Trigonometric sums for correlation between sextupoles of the same family:

```
tr[i_,phi_,ns_]:=(ns Sin[mm[i]]-Sin[ns mm[i]]+(1-Cos[ns mm[i]])*
        (Cos[pmq[i]]+Cos[pmq[i]-2m[i].phi-(ns-1) mm[i]])/
        Sin[pmq[i]])/(1-Cos[mm[i]]);
```

and between sextupoles of the different families:

```
trs[i_]:=(-Cos[pmq[i]-(ns1+.5) mm[i]]+Cos[pmq[i]-.5 mm[i]]+
         Cos[pmq[i]-2m[i].phi1-(ns1-1.5) mm[i]]*(1-Cos[ns1 mm[i]]))/
         Sin[pmq[i]]/(1-Cos[mm[i]])+ns1/Sin[.5 mm[i]];
```

Detuning coefficients:

```
dq1de1:=-(
      k211^2*bx1^3*(tr[4,phi1,ns1]+3*tr[1,phi1,ns1])+
      k212^2*bx2^3*(tr[4,phi2,ns2]+3*tr[1,phi2,ns2])+
      2*k211*k212*bx12^3*(trs[4]+3*trs[1])
      )/64/Pi*nsuper;
dq1de2:=-(
      k211^2*bx1*by1*(-bx1*tr[1,phi1,ns1]+.5*by1*
```

```
        (tr[2,phi1,ns1]-tr[3,phi1,ns1]))+
      k2l2^2*bx2*by2*(-bx2*tr[1,phi2,ns2]+.5*by2*
        (tr[2,phi2,ns2]-tr[3,phi2,ns2]))+
      k2l1*k2l2*bxl2*(-(bxl*by2+bx2*byl)*trs[1]+
        byl*by2*(trs[2]-trs[3]))
        )/16/Pi*nsuper;
dq2de2:=-(
      k2l1^2*bxl*byl^2*(tr[1,phi1,ns1]+
      (tr[2,phi1,ns1]+tr[3,phi1,ns1])/4)+
      k2l2^2*bx2*by2^2*(tr[1,phi2,ns2]+
      (tr[2,phi2,ns2]+tr[3,phi2,ns2])/4)+
      2*k2l1*k2l2*bxl2*byl*by2*(trs[1]+(trs[2]+trs[3])/4)
      )/16/Pi*nsuper;

gr=Plot3D[ dq1del/1000, {mux,124,141},{qx,124.3,125.3},
BoxRatios->{1,1,1}, PlotPoints->30];
```

■ Resonance excitation

The term in the Hamiltonian, exciting the (i-j)*qx+(k-l)*qy=n0 resonance, may be represented as a product of numerical coefficient rijkl and Cos[m.delta-n0*theta-Pi/2*Apply[Plus,m]]*Ix^((i+j)/2)*Iy^((k+l)/2), where m={i-j,k-l}, delta is a list of angle variables (see Ref.[9]), Ix and Iy are the action variables.

For performing the Fourier analysis some geometry parameters are needed: superperiod and cell lengths [m]:

```
lsuper=6664.72; lcell=79.;
```

distance from the IP to the first sextupoles in the families [m]:

```
ls1=482.46; ls2=ls1-lcell/2;
```

Corresponding angular values:

```
thel1=2*Pi*lcell/lsuper; thetl=2*Pi*ls1/lsuper;
thet2=2*Pi*ls2/lsuper;
```

First order (in the sextupole strength) resonance driving terms.

```
alf[i_]:=mm[i]+(n0-m[i].q)*thel1;
cont[i_,phi_,thet_,ns_]:=Sin[alf[i]/2*ns]/Sin[alf[i]/2]*
Cos[m[i].phi+(n0-m[i].q)*thet+(ns-1)*alf[i]/2]/4*Sqrt[2]/Pi*nsuper;

cs[2]=-1/2.; cs[3]=-1/2.; cs[4]=1/6.; bxls=Sqrt[bxl]; bx2s=Sqrt[bx2];

r3000:=cs[4]*(k2l1*bxls^3*cont[4,phi1,thetl,ns1]+
            k2l2*bx2s^3*cont[4,phi2,thet2,ns2]);
r1020:=cs[2]*(k2l1*bxls*byl*cont[2,phi1,thetl,ns1]+
            k2l2*bx2s*by2*cont[2,phi2,thet2,ns2]);
r1002:=cs[3]*(k2l1*bxls*byl*cont[3,phi1,thetl,ns1]+
            k2l2*bx2s*by2*cont[3,phi2,thet2,ns2]);
r2100:=cs[4]*(k2l1*bxls^3*cont[1,phi1,thetl,ns1]+
            k2l2*bx2s^3*cont[1,phi2,thet2,ns2])*3;
r1011:=cs[3]*(k2l1*bxls*byl*cont[1,phi1,thetl,ns1]+
            k2l2*bx2s*by2*cont[1,phi2,thet2,ns2])*2;
qx=125.23;
plt1=Plot[{dq1del/1000,r3000},{mux,125,140},
PlotStyle->{Thickness[.003],Dashing[{.05,.025}]},
Ticks->{{125,130,135,140}, Automatic}];
plt2=Plot[{dq1del/1000,r3000},{mux,100,115},
PlotStyle->{Thickness[.003],Dashing[{.05,.025}]},
Ticks->{{100,105,110,115}, Automatic}];

Exit[];
```